DESIGN OF A SI CUK CONVERTER BASED ON BRIDGELESS POWER FACTOR CORRECTION WITH REGENERATIVE BRAKING

Shilpa Jadhav

Access Online

Article DOI:
10.5281/zenodo.21413465

Department of Electrical and Electronics Engineering, Shetty Institute of Technology, Kalburgi

How to Cite:
Shilpa Jadhav (2026), Design of A Si Cuk Converter Based on Bridgeless Power Factor Correction with Regenerative Braking, International Educational Journal of Science & Engineering (IEJSE),Vol: 9, Special Issue, May 2026 325-332

ABSTRACT

When the bridge in an electric vehicle charging system is eliminated, the volume of a switching inductance (SI) powered Cuk converter is reduced with an enhanced power factor. Traditional battery charging methods entail two stages ofpower conversion. The voltage ratio of conversion is increased by the one stage switching inductor architecture. Once the converter's performance in both steady state and transient scenarios is noted, an excessive gain bidirectional converter is added to power the motor for an electric car. The simulation work is done using MATLAB/Simulink software. A hardware prototype is made to confirm that the proposed system functions as anticipated.

KEYWORDS: Cuk Converter, Power Factor Correction, High Gain Converter, Regenerative Braking

I. INTRODUCTION

Since the percentage of demand for LEVs is steadily rising, customers and power distributors alike are eagerly awaiting the charging station equipped with the best technique for enhancing power quality. An unregulated rectifier, a dc bus capacitor, and an isolated or non-isolated dc-dc converter are often the starting points of the present generation of LEV chargers. When DBR and a large dc-link capacitance are used together, they draw altered electrical current from the electrical source that is high in harmonics, which negatively affects the supply's electrical power factor (PF) and the overall efficiency of the system. These short comings in traditional low-wattage rating converters are mostly eliminated by power factor correction, or PFC.

A dc-dc converter is used in an APFC technique to enhance the power quality of the converter's source side, situated between DBR and CDC. It is important to realize that an APFC conversion may accomplish a number of functions in a charger, regardless of which one is a single-stage or two-stage converter with various layouts. An APF cuk conversion is used in a two-stage system to meet source requirements, and an additional dc-dc converter is needed to meet load requirements. Nevertheless, just one APF cuk converter in a single-stage converter satisfies both requirements.

Regarding the reason of recharging EVs and LEVs, a variety of two-phase converters designs based on different APFC approaches have been investigated. Regarding component count, conductivity and switching expenditures, control level of complexity, and efficacy, each approach has advantages and disadvantages. A number of bridgeless APFC converter featuring either partial or total DBR deletion have been documented in the literature in an effort to increase efficiency by lowering losses in conduction on the APF cuk transformation stage. A thorough examination of bridgeless The presentation includes an APF cuk converter. Recently, particular bridgeless incorporated recharging methods have been proposed as a means of maintaining

Research Paper

the benefits of two-stage converters with fewer components and charging limitations. By integrating the power electronic equipment, total device count and related losses are decreased.
\
However, their decreased attractiveness for LEV applications might be attributed to the increasing control difficulty and high gadget stresses. One of the main benefits of the two-phase conversion is that it provides ripple-free recharging current. Several writers have claimed that when low-frequency variations in the driving current are appropriately controlled, they have no effect on the battery's performance. Many academics have suggested alternative single-stage conversion architectures for EVs and LEVs together with improved quality of power at the supply side to overcome these problems with two-phase conversions.

The single-stage converters have an easily understood control architecture, a high power density, and few components. When compared to a two-stage converter, a well-designed single-stage converter system may also offer higher efficiency. The limited output voltage capabilities of the conventional boost converter and the significant supply current distortion of the common buck converter preclude their use in the role of APFC for single-stage LEV conversions. Therefore, using buck-boost developed converters usually eliminates the drawbacks of using buck and boost based converters.

The lowest amount of current between the input and output fluctuation is seen in buck-boost dc-dc converters, namely in the Cuk model. However, because of their limited gain capabilities, classic buck-boost converters that convert DC to DC are less suited for delivering a transformer less single-stage transformation for the LEVs. The transformer less converter structure in LEVs runs at a very low duty cycle because of the reduced battery voltage, which ultimately compromises the charging system's flexible effectiveness and efficacy.

The voltage strain among the pieces is further increased by the transformer's leakage impedance. Academic discourse rarely addresses the transformer less converter design for plug-in vehicles (LEVs) that is founded on enhanced quality of power. The latest developments include coupling inductors, converter a cascade of interleaved interface architectures, substituted inductive devices, and dual switching inductor-capacitor architecture. On the other hand, the coupling coefficient strongly influences the converter's operation variables when there are connected inductive devices.

When adapting for rising voltage and currents trains, the quadratic converter performs better than a cascaded converter. A transitioning split circuit made up of a couple of diode semiconductors separated type inductive elements, or capacitors is suggested as a solution to these problems. Because of the CCM procedure, this charging device has bigger magnetically charged elements, a complicated control system, and a high cost.

This work proposes an improved single-stage modified power factor converter based on a modified Cuk converter. The dcm method function makes the control system implementation simple because it does not require any sensors. The bridgeless architecture of the conversion device leads to a notable decrease in the total number of elements utilized. Employing both constant voltage and constant current methods of control under varied voltage source circumstances, the suggested converter is tested. A significant gain reversible conversion device powers the motor after the car is powered by batteries. Since it's bidirectional, regenerative braking may be applied to increase the vehicle's riding duration.

II. SYSTEMDESCRIPTION

The proposed system is provided below in Fig1

Fig. 1: Proposed system Blockdiagram

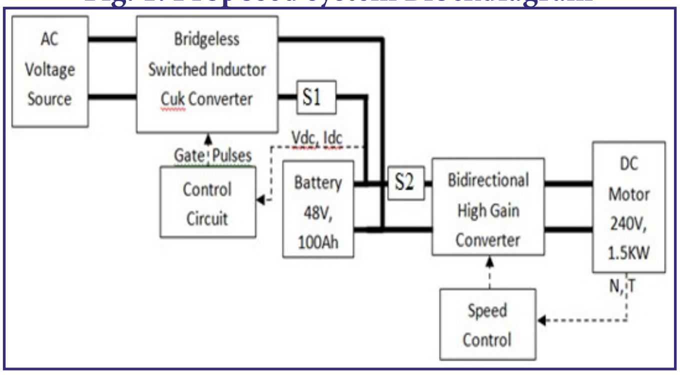

In this instance, the BSIC converter is attached to the ac supply when the car is charging in order to charge the battery when the primary switch (S1) is

turned on while switch 2 (S2) is turned off. In this case, the load is the battery. The battery's voltage and current are managed via the control loop. When the car starts, S1 is turned off (the ac supply is unplugged) while S2 is turned ON (the electric motor is engaged). In this case, the power source is the battery. The DC motor's measured speed is passed onto the speed regulation loop, that modifies the reversible converter's voltage output to bring the speed measured closer to the target speed.
BSIC Converter and Control:

The bridgeless Cuk converter circuit is provided below:

Fig. 2 : circuit diagram for Single phase Single Stage Bridgeless switched Inductor Cuk Converter (BSIC)Power Factor Correction (PFC) Converter

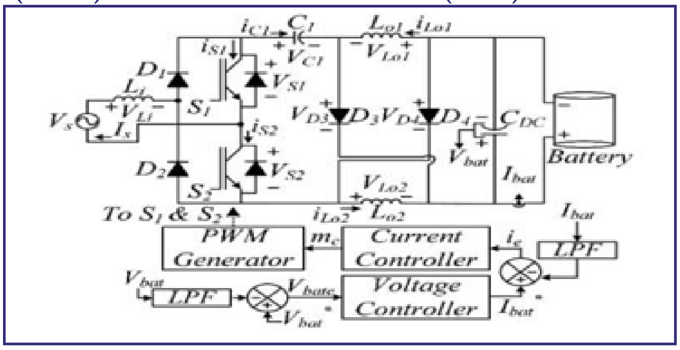

Regarding the LEV charging implementation, this arrangement provides a single-stage ac-dc conversion with excellent power quality and high voltage transformation capacity on the power source side. The single-phase units source which drives the bridgeless structure on the outermost end has a nominal voltage rating of 220 V, 50 Hz (Vs). Together with acting as a slope with the input current (Is), the supply inductor (Li) also functions to serve as the Cuk converter's feed inductance.

Dual dynamic switches, S1 and S2, make up the remaining limb of the rectifying bridge, whereas diodes that are D1 and D2, make up the first leg. This is not the same as the conventional DBR, which is made up of four diodes together. To minimize controller complexities. D1 and D2 work throughout every one of the two different half-cycles of the source voltage, accordingly, whereas the switching elements (S1 and S2) operate concurrently irrespective of the power source's polarity.

A SI network that includes two diodes (D3 and D4) and a pair of inductances (Lo1 and Lo2) is offered on the load side. The charging the ends of inductive devices in sequence and draining them in parallel increases the charger's overall gain. The load is a battery featuring a voltage rating of 48 V and 1.3 Ah. Using the fewest amount of sensing devices to accomplish the charger's control both simplifies and lowers the cost of the conversion device control. The following list includes the aforesaid converter's operational modes:

Mode1:

Fig. 3: Mode one operation of BSIC

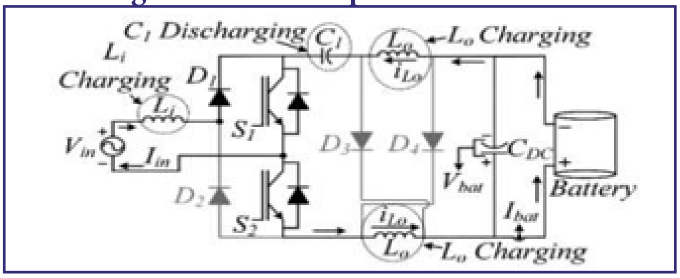

In this, the source side inductance and both power electronicswitchesS1andS2areinoperation.With the help of the input voltage source, Li is being charged, while C1 is being discharged to supply power to the inductors Lo and battery.

Mode2:

Fig. 4: Operation of Mode2 of BSIC

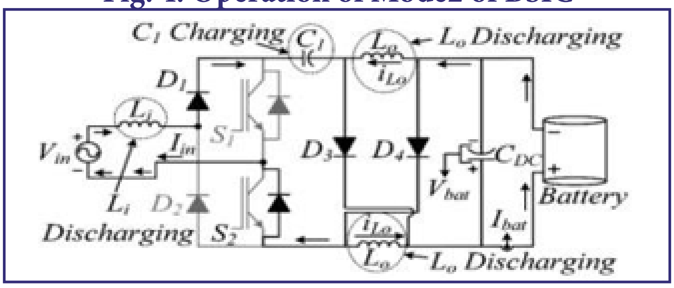

In this case, the input side inductor begins to discharge while both power electronic switches are in the OFF state. Along with conducting is the body diode of S2, the diodes D1, D3, and D4. While the inductors Lo are discharging, the capacitor C1 begins to charge.

Mode3:

Fig. 5: Operation of Mode3 of BSIC

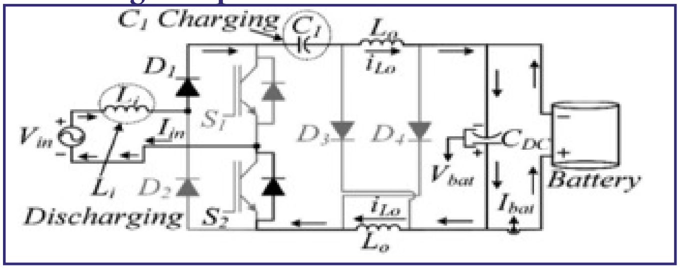

The diodes D3 and D4 stop conducting because of the reverse bias. While C1 is still charging, the input side inductance Distills charging. The inductors' Lo state allows the current to freely flow through them without being charged or discharged. The voltage conversion ratio of the cuk converter is provided below

where D1 represents the diodes(D5andD6) duty ratio and M= V bat/Vin.

The load side inductance value is calculated as provided below

$$V_{\text{bat}} = V_{\text{in}} \cdot D/(2 * D_1) = M \cdot V_{\text{in}}.$$

The sources inductance value is calculated for CCM is provided below:

$$L_{o\text{critical}} = R_{L\,\text{min}} / \left[f_s \cdot (1 + 2 \cdot M_{\text{max}}) \right]$$

The value ofC1 is calculated as

$$C_1 = 1/\left\{ \omega_{res}^2 \cdot (L_i + L_{o1} + L_{o2}) \right\}$$

$$L_{i\text{critical}} = \frac{V_{\text{inmax}}^2 \cdot D_{\text{max}}}{P_{\text{max}} \cdot \chi \cdot f_s} = \frac{(\sqrt{2} \cdot V_{\text{smax}})^2 \cdot D_{\text{max}}}{P_{\text{max}} \cdot \chi \cdot f_s}$$

where is resonant frequency CDC is calculated as

$$C_{DC} = P_{\text{max}} / (4\pi \cdot f_{Line} \cdot \lambda \cdot V_{\text{batmax}}{}^2)$$

HIGH GAIN BOOST CONVERTER

Similar to a resistor, an inductor behaves as an appliance and uses energy when it is charged, and when it is discharged, it acts as a source of energy. Because the voltage it creates during the phase of discharge is based on the rate of current change rather than the starting charging voltage, a variety of voltages at the input and output are possible. The following graphics shows the basic lay out for a boost converter with a high voltage conversion ratio:

Fig. 6: Basic configuration of high gain boost converter

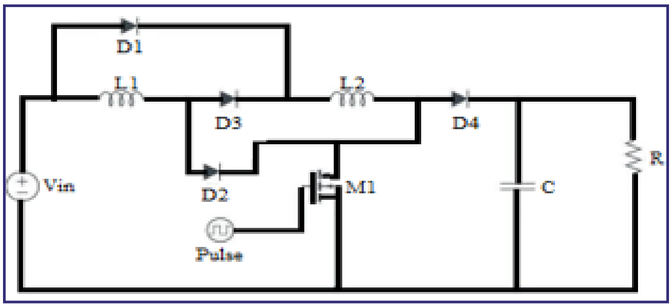

The proposed converter operates in one of two modes while the power electronic switch S is in operation and in both modes when switch S is turned off. Inductors L1 and L2 get charged simultaneously by the source voltage Vin through Diodes D1 and D2, respectively, when switch S is switched ON. A single capacitor, four diodes, and a MOSFET switch with a PWM switching rate make up the power circuit approach. Capacitor C is discharged by the load. D3 and D4 reverse biased diodes were available. The operation is depicted in the accompanying figure while switch S is turned ON.

Fig. 7: operation of converter when switch is ON.

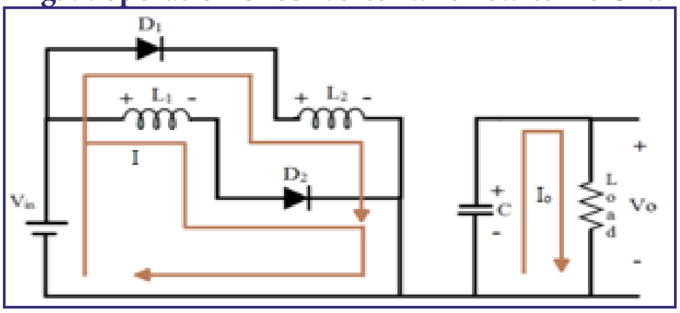

Both inductors are draining while the power electronic switch S is turned off, and the voltage source is connected in series by diodes D3 and D4. D1 and D2 are not conducting at this time.

Fig. 8: operation of converter when switch is OFF.

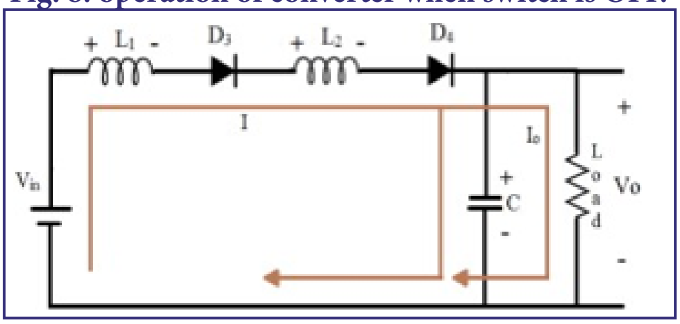

The design equations for the high gain dc-dc converter is provided below:

$$\frac{V_o}{V_{in}} = \frac{1 \pm D}{1 - D}$$

The inductor value is provided by the relation shown below

$$\Delta I_L = (0.2 \text{ to } 0.4) \times I_{OUT(max)} \times \frac{V_{OUT}}{V_{IN}}$$

The load capacitor value is calculated as follows

$$L = \frac{V_{IN} \times (V_{OUT} - V_{IN})}{\Delta I_L \times f_S}$$

Where ΔVOUT = desired output voltage ripple. Switches Q2 and Q3 are used in place of the diodes D2 and D3 for bidirectional power flow; Q3 works at a PWM frequency while Q2 operates at a lower frequency solely to provide a path for the load (the battery serves as the load during regenerative braking)..

Fig. 9: circuit diagram of converter when diodes replaced with switches Q1&Q2

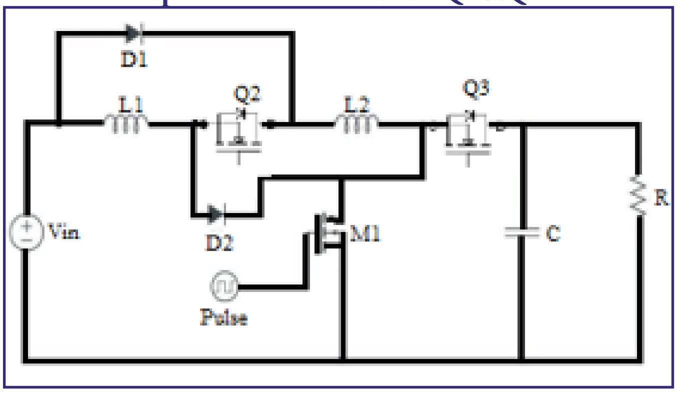

CONTROL STRUCTURE OF BSIC CONVERTER

The suggested converter is used to control the battery's charging current in both CC and CV modes, depending on the circumstance. While the outer loop controls variations in Vbat, the inner loop controls Ibat and maintains UPF operation with the least amount of distortion. The reference battery current (Ibat) is obtained by matching the Vbat and Vbat for the outer loop, and the error (Vbate) is fed into the proportional-integral (PI) control as an input. The voltage PI controller's output serves as Ibat. The specified outer loop expressions are

$$I^*_{\text{bat}}(k) = I^*_{\text{bat}}(k-1) + k_{pV}\{V_{\text{bate}}(k) - V_{\text{bate}}(k-1)\} + k_{iV} \cdot V_{\text{bate}}(k)$$

where kpV stands for the proportional gain of the voltage PI controller, kiV for the integral gain, andk for the sampling moment. Inner loop control is implemented by comparing the current used to charge Ibat to Ibat, and sending the error (Ie) to the control circuit after that. The needed duty ratio (mc) is provided by the PI controller's output as

$$m^*_c(k) = m^*_c(k-1) + k_{pI}\{I_e(k) - I_e(k-1)\} + k_{iI} \cdot I_e(k)$$

where kpI and kiI, respectively, are the gains of the current PI controller. Next, the duty ratio (mc) is compared to a carrier waveform. Switch (S1 andS2) receive the relevant gate drive signals from the comparison. SPEED CONTROL STRATEGY

The DC reference voltage (v*dc) is provided below is calculated with the help of reference speed.

$$V^*_{dc} = k_v \omega^*$$

The reference voltage (v*dc) is compared with the actual load voltage (v*dc) and the error voltage (v*dc) is provided below as

$$V_E = V^*_{dc} - V_{dc}$$

The generated error is given to proportional–integral (PI) control, which provides the reference voltage v*dc as follows

$$V_C(k) = V_C(k-1) + K_P \{V_E(k) - V_E(k-1)\} + K_i V_E(k)$$

The pulses generated for the boost converter is as follows

{IfFM<vgating pulse is HIGH}

{IfFM≥Vgating pulse is LOW}

III. SIMULATION SETUP & RESULTS

The simulation parameters for the proposed converter are shown below in Table I:

Input Voltage	(160-230)V
Input power	1500W
Switching Frequency	2 KHZ
Inductor	9.1mH
Coupling Capacitor	55.6µF
Output Capacitor	2mF
Battery voltage	48V
Battery capacity	1.5Ah
DC Motor parameters	150V, 500W, 1500rpm

The simulation circuit for the cuk converter with PI controller is provided below:

Fig. 10: PI controller

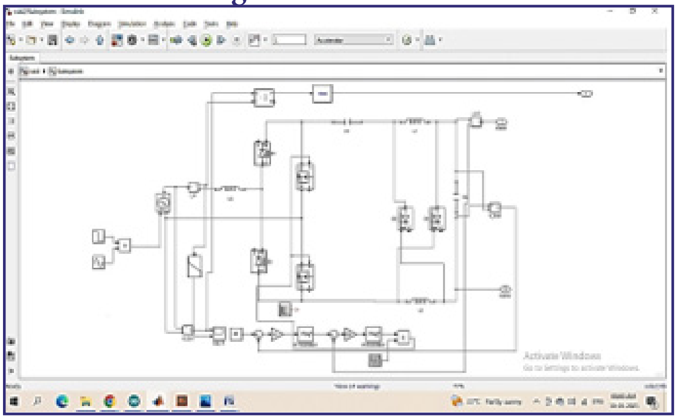

In this, the supply voltage of 230V is applied to the proposed converter from t=0 to t=0.3s. Then the supply changed from 230V to 160V at t=0.3s. During these two modes, the battery will be charging and the motor will be in standstill condition. The simulation circuit for the high gain bidirectional converter with PI controller is provided below:

Fig. 11: Bridges

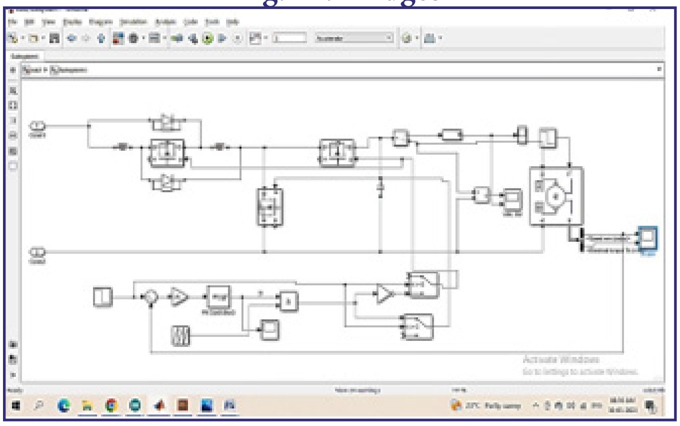

The motor begins to function in the forward direction and the battery begins to discharge at t=0.6s (mode 3). Regenerative braking is performed to the motor at t=0.95s (mode 4), and the charge stored in the motor windings is extracted to recharge the battery.

In mode1 and 2, the supply is connected and charges the battery of the EV. The supply voltage and current is provided is provided below:

Fig. 12: Wave form of Voltage and Current

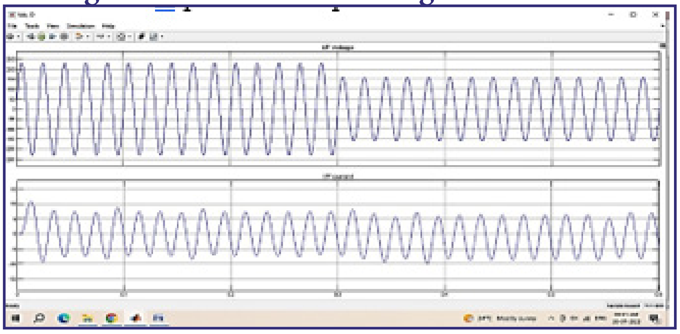

The supply voltage in this is around 220V and 7A. The supply charges the battery, and the wave forms of its voltage and % SOC are shown below:

Fig. 13.Supply voltage wave form

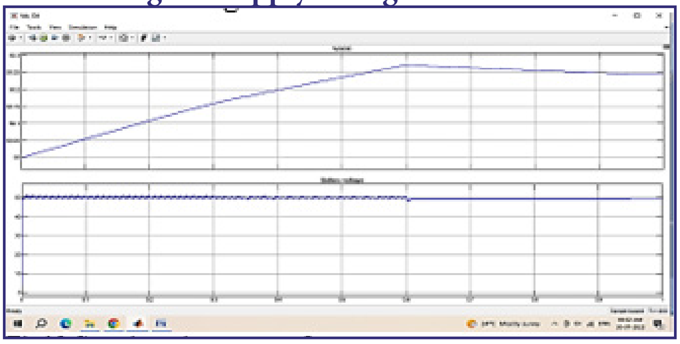

This keeps the battery voltage at 52V (which is greater than the 48V battery nominal voltage), and the SOC percentage is rising. At t=0.6s, the supply is cut off, and as the battery begins to discharge and deliver power to the car, the %SOC starts to fall. Below are the motor voltage and current values:

Fig. 14: Charge and discharge ON battery

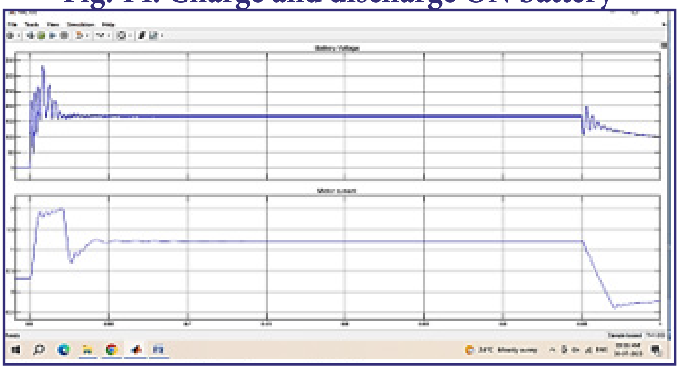

At t=0.6s, the motor begins to run in the forward direction with a positive current flow, and at t=0.95s, regenerative braking is performed with a negative current flow, or it is supplied back to the battery to charge it. Below is a list of the battery

VOLTAGE AND %SOC DURING REGENERATIVE BRAKING:

Fig. 15: SOC and SOD wave forms

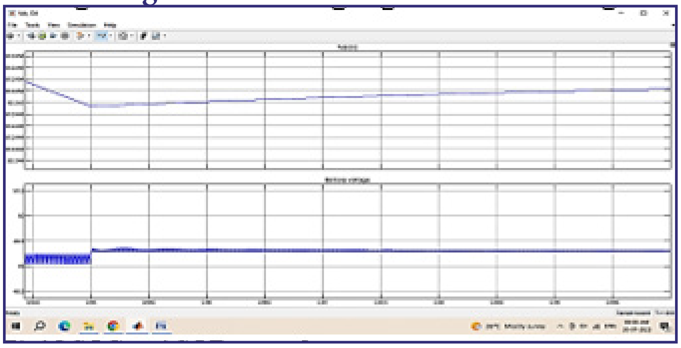

The battery is first charged by the source until t=0.6s, resulting in a high battery voltage and rising SOC. The soc starts to decrease as the engine turns on at time t=0.6s as a result of battery discharge. Regenerative braking is used at time 0.95 seconds, which recharges the battery once more and raises the voltage and %SOC. The %THD of the supply current is provided below:

Fig. 16.THD at 2.01%

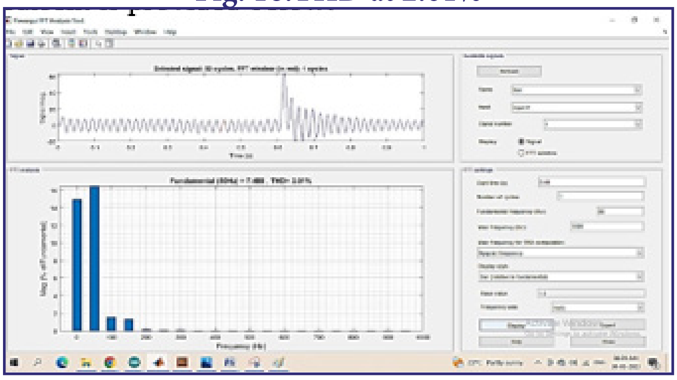

The %THD of the supply current is around 2.01%. The efficiency of the proposed system is provided below:

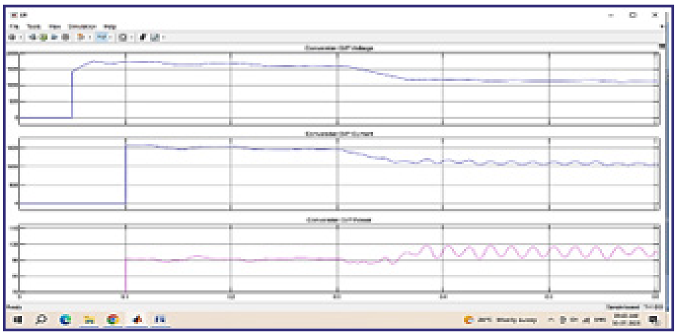

With an efficiency of about 95%, the input power is in the range of 1570W, and the output power is about 1500W.

Using a battery of 12V, 2.2Ah and a BSIC converter with an output voltage of 24V, 50 Hz, a hardware prototype model of the proposed

converter is created. When the battery is being discharged, the input voltage of the battery is 12V, and the load voltage of the high gain converter is 48V. ThehardwarespecificationsarelistedinTable II below.

In battery discharging mode, the battery voltage is provided as input and the load voltage is provided below:

TABLE II: Hardware Parameters

IRF 250N - MOSFET	200v, 30A
U1560-DIODE	200-400-600v, 15a
Capacitor	1000µF, 25V 1000µF, 100V
TRANSFORMER	12V, 1A
TLP 250 – DRIVER IC	12V, 1.5A
CD 4050 BUFFER IC	3-18V, 0.32mA
12V REGULATOR 7812	12V, 1A
IN 4007 DIODE	700V, 1A
ARDUINO UNO CONTROLLER	7-12V, 20mA

The suggested converter uses an Arduino uno control to generate the pulses, which are then sent to the driver circuit (TLP 250) to drive the mosfets IRF 250. Below are the input voltage waveforms:

Fig. 17.Input wave forms

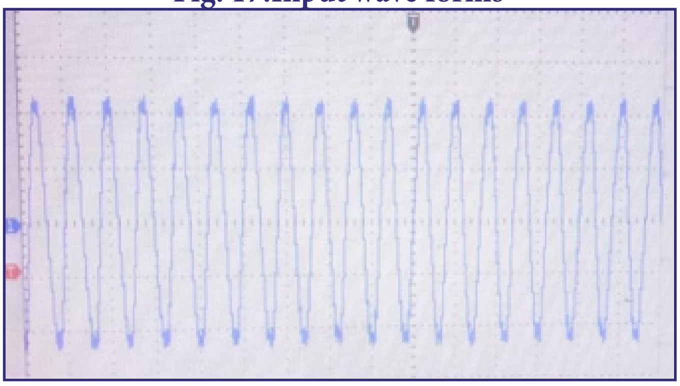

In this the voltage division is 10V/div and the input voltage is around 24V. It is provided to charge the battery. The battery voltage is provided below:

Fig. 18: Battery discharge voltage

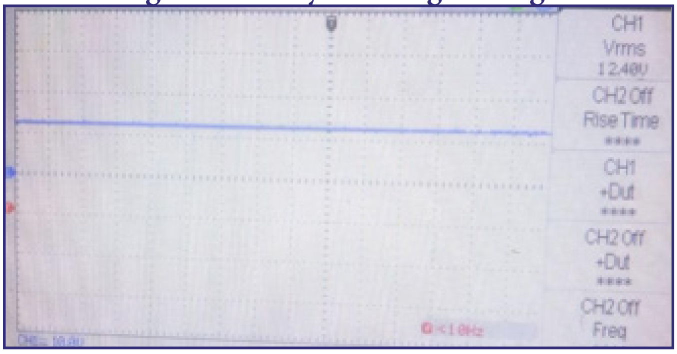

Fig. 19: The load voltage of the high gain converter is around 40.4V

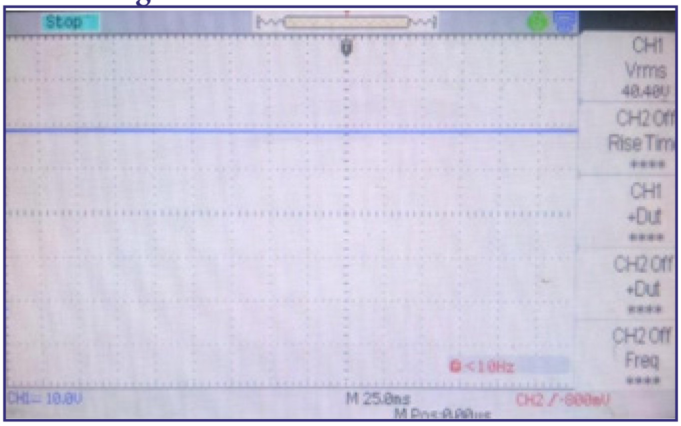

Fig . 20: prototype model of proposed converter

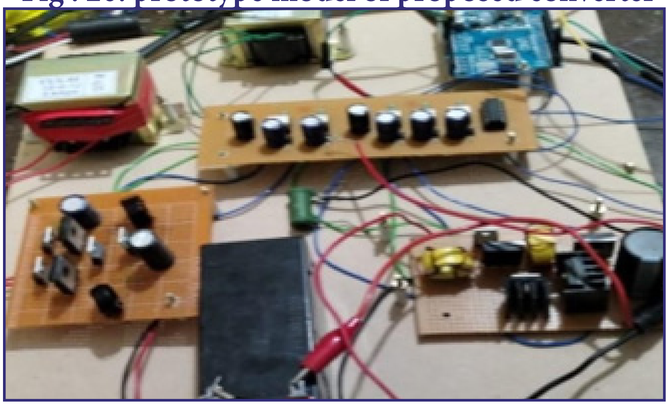

IV CONCLUSION

The size of the converter is decreased as the bridge is removed from the switched inductor (SI) based Cuk converter that was designed in this research for use with electric vehicles. A high gain bidirectional converter is introduced to power the motor for the operation of an electric vehicle after the performance of the converter under steady state and transient situations is noted. Regenerative braking is used to extend the vehicle's range by restoring energy from the motor to the battery. The simulation results show that the proposed converter is 95% efficient. A hardware prototype model was created, and the suggested system's functionality was checked.

REFERENCES

1. L. Lachvajderovaand J. Kadarova, "Analysis of internal combustion engine vehicle, battery electric vehicle and emissions from transport," Transp. Logistics, vol. 21, pp. 21–33, Dec. 2021.
2. L. Wang, Z. Qin, T. Slangen, P. Bauer, and T. van Wijk, "Grid impact of electric vehicle fast charging stations: Trends, standards, issues and mitigation measures—An overview," IEEE Open J. Power Electron., vol. 2, pp. 56–74, 2021, doi:10.1109/OJPEL.2021.3054601.
3. Bahrami, "EV charging definitions, modes, levels, communication protocols and applied standards," Changes, vol. 1, pp. 1–10, Jan.2020, doi: 10.13140/RG.2.2.15844.53123/11.
4. L. I. Dulau and D. Bica, "Effects of electric vehicles on power networks," Proc. Manuf., vol. 46, pp. 370–377, Dec. 2020, doi: 10.1016/j.promfg.2020.03.054.
5. M. R. Khalid, I. A. Khan, S. Hameed, M. S. J. Asghar, and J.-S. Ro, "A comprehensive review on structural topologies, power levels, energy storage systems, and standards for electric vehicle charging stations and their impacts on grid," IEEE Access, vol. 9, pp.128069–128094,2021, doi:10.1109/ACCESS.2021.3112189.
6. M. K. Das and S. K. Jain, "Review on optimization techniques used for scheduling of electric vehicle charging," in Proc. Int. Conf. Control, Autom., Power Signal Process. (CAPS), Dec.2021, pp.1–6, doi:10.1109/CAPS52117.2021.9730621.
7. S. Rivera, S. Kouro, S. Vazquez, S. M. Goetz, R. Lizana, and E. Romero-Cadaval, "Electric vehicle charging infrastructure: From grid to battery," IEEE Ind. Electron. Mag., vol. 15, no. 2, pp. 37 51, Jun. 2021, doi: 10.1109/MIE.2020.3039039.
8. S. Habib, M. M. Khan, F. Abbas, L. Sang, M. U. Shahid, and H. Tang, "A comprehensive study of implemented international standards, technical challenges, impacts and prospects for electric vehicles," IEEE Access, vol. 6, pp. 13866–13890, 2018, doi:10.1109/ACCESS.2018.2812303.
9. J. A. Sanguesa, V. Torres-Sanz, P. Garrido, F. J. Martinez, and J. M. Marquez-Barja, "A review on electric vehicles: Technologies and challenges," Smart Cities, vol. 4, no. 1, pp. 372–404, Mar.2021, doi: 10.3390/smartcities4010022.
10. M. Safayatullah, M. T. Elrais, S. Ghosh, R. Rezaii, and I. Batarseh, "A comprehensive review of power converter topologies and control methods for electric vehicle fast charging applications," IEEE Access, vol.10, pp.40753–40793,2022, doi: 10.1109/ACCESS.2022.3166935.